

Combined optimization of a wind farm and a well field for wind-enabled groundwater production

E. Annette Hernandez · Venkatesh Uddameri · Sreeram Singaraju

Received: 24 May 2013 / Accepted: 28 October 2013 / Published online: 8 December 2013
© Springer-Verlag Berlin Heidelberg 2013

Abstract Energy requirements constitute a significant cost in groundwater production and can also add to a large carbon footprint when fossil fuels are used for power. Wind-enabled water production is advantageous as it minimizes air pollution impacts associated with groundwater production and relies on a renewable resource. Also, as groundwater extraction represents a deferrable load (i.e., it can be carried out when energy demands within an area are low), it provides a convenient way to overcome the intermittency issue associated with wind power production. Multiple turbine wind farms are needed to generate large quantities of power needed for large-scale groundwater production. Turbines must be optimally located in these farms to ensure proper propagation of kinetic energy throughout the system. By the same token, well placement must reconcile the competing objectives of minimizing interferences between production wells while ensuring the drawdowns at the property boundary are within acceptable limits. A combined simulation–optimization based model is developed in this study to optimize the combined wind energy and water production systems. The wind farm layout optimization model is solved using a re-sampling strategy, while the well field configuration is obtained using the simulated annealing technique. The utility of the developed model is to study wind-enabled water production in San Patricio County, TX. Sensitivity analysis indicated that identifying optimal placement of turbines is vital to extract maximum wind power. The variability of the wind speeds has a critical impact on the amount of water that can be produced. Innovative technologies such as

variable flow pumping devices and aquifer storage recovery must be used to smooth out wind variability. While total groundwater extraction is less sensitive to uncertainty in hydrogeological parameters, improper estimation of aquifer transmissivity and storage characteristics can affect the feasibility of wind-driven groundwater production.

Keywords Water energy nexus · Total dissolved solids · Brackish groundwater · Energy

Introduction

Groundwater resources are more easily accessible and reliable than surface water resources in most arid and semi-arid regions of the world. The over-appropriation of surface water resources and increased awareness of environmental and ecological services, provided by rivers coupled with their sensitivity to climate change, have resulted in a greater push towards the use of groundwater resources in recent years. Shallow groundwater supplies are susceptible to anthropogenic pollution (Uddameri and Honnunar 2007) and are affected to a greater degree by climatic phenomenon [Uddameri et al. 2013 (in press)]. Shallow groundwater systems interact with surface water bodies, provide baseflows and sustain riparian ecosystems (Sophocleous 2002). Furthermore, shallow aquifer systems are tapped extensively by small users for meeting rural, domestic, and livestock uses; and large-scale production can lead to drying up of wells and spring flows, and, as such, pose both economic as well as ecological risks. Deeper aquifer formations are noted to not be influenced by climatic phenomenon (Uddameri 2007) and are seen to be more reliable sources of water supplies for large-scale uses. By the same token, new groundwater users (e.g., for

E. A. Hernandez (✉) · V. Uddameri · S. Singaraju
Department of Civil and Environmental Engineering, Texas
Tech University, Box 41023, Lubbock, TX 79409, USA
e-mail: annette.hernandez@ttu.edu

hydraulic fracturing operations) may be required to obtain their water from deeper sources to avoid the above stated economic and environmental externalities.

Deeper aquifers are typically under confined conditions and have considerable hydrostatic pressure; as such, the potentiometric surface is higher than the top of the deeper aquifer. However, hydrostatic pressure loss is to be expected as greater amounts of groundwater are withdrawn from the aquifer. The lifting of water from the deeper formation to the surface requires considerable energy which increases over time as these aquifers are not readily recharged. Energy costs, therefore, form a major factor in producing groundwater from deeper formations (NAP 1997). The volatility of the fossil-fuel-based energy market adds a significant level of uncertainty to the long-term planning of groundwater resources from deeper aquifer formations. By the same token, reliance on these fossil-fuel-based energy sources for water production has other environmental consequences, such as an increased carbon footprint and air quality issues [Hernandez et al. 2013 (in press)]. Therefore, while the usage of deeper aquifers for groundwater production has certain economic and environmental benefits, it can also have negative economic and environmental consequences arising from the need for a greater amount of energy for lifting water.

The use of renewable and cleaner energy technologies for lifting water provides a way to overcome some of the economic and environmental disadvantages of producing groundwater from deeper aquifers. Coastal areas generally have favorable winds due to atmospheric instabilities at the coastal-land boundary (Barthelmie 1999). Wind resources offer a cleaner alternative to fossil-fuel-based energy production and as such have a smaller carbon footprint and do not cause air quality issues. However, wind speeds exhibit considerable spatial and temporal variability which makes reliable forecasts of available wind resources a challenging task (Monteiro et al. 2009). In addition, wind energy cannot be stored readily and the possibility of having low winds during high-energy needs calls for innovations in managing wind resources (Black and Strbac 2007). There is a growing interest in storing wind energy in the form of water. The coupling of wind power production with hydropower production has been an active area of interest in recent years (Castronuovo and Lopes 2004; Benitez et al. 2008). As short-term storage of groundwater can be easily accomplished, the production of groundwater can be viewed as a deferrable energy load. Groundwater can be produced when winds are high and when demands on the produced energy are low and stored for later use. The concept of using wind resources for groundwater extraction is not completely new. Small-scale windmills are ubiquitous in South Texas and many other rural areas of the world and are used to extract small amounts of water from

shallow aquifers for satisfying domestic and livestock needs. For large-scale production, this technology needs to be up-scaled using modern day wind turbines that convert wind energy to electrical energy, and cylindrical pumps must be replaced with more powerful and reliable submersible centrifugal pumps that overcome problems with cavitation that arise when the elevation between the pump and the fluid level is large. An array of wind turbines (wind farm) becomes necessary when the energy requirements are high; and, in a similar fashion, water quality and specific capacity constraints will warrant multiple groundwater wells for producing the necessary water to meet demands.

Wind turbines extract energy from incoming wind streams, which result in the formation of a wake and turbulence in the downwind direction. Improper placement of wind turbines results in a greater loss of efficiency and diminishes the overall energy production. Therefore, characterization of the wake effects as well as optimization of wind farm layouts, in recent years, has been an active area of research (Chowdhury et al. 2012; Gonzalez-Longatt et al. 2012). In particular, analytical wake models have been combined with evolutionary optimization models for identifying wind farm layouts that lead to maximization of wind energy (Grady et al. 2005; Elkinton et al. 2008; Kusiak and Song 2010; Gonzalez et al. 2010; Chowdhury et al. 2012). Generally speaking, the wind farm layout model uses a simulation model to characterize wake effects and the velocity deficits and couples it with an optimization routine to identify the best subset of possible wind turbine sites within a given area of interest; and therefore, from a mathematical standpoint, represents an unconstrained mixed-integer nonlinear optimization problem.

In a similar vein, a groundwater well field consists of several wells. Groundwater well fields are not only required to produce necessary amounts of water but are also useful to regulate water quality, particularly of trace elements. Proper spacing between the wells is necessary to avoid interference effects and ensure minimal overlap between the cones of depressions of individual wells. Therefore, from a field development standpoint, wells must be spaced as far apart as possible. In addition to water quality and geologic factors which control the production capacity at the well, the spacing is also constrained by any drawdown policies that are enforced at the boundaries. In most areas, the drawdown at the boundary of the well field cannot be more than what is to be expected due to natural variability in hydraulic heads.

The energy generated at each wind turbine is sent to a collector substation where it is aggregated and tied into a grid and transmitted to meet an electrical power load requirement. The pump at each well represents a load. In a similar manner, water at different wells is collected and transmitted to a treatment facility for distribution. While

maximizing the spacing between the wells is warranted to achieve minimal interference, it also adds energy requirements, as water pumped at the well has to be piped to a central collection facility. Distributed electric loads result in voltage drops and energy losses during transmission. Thus, from an energy efficiency standpoint, it is better to keep the wells as close as possible. However, doing so results in higher drawdowns at each well due to well interferences, which, in turn, increases the lift required and hence the energy requirements. Therefore, optimal operation of wind-enabled groundwater production represents a careful balance between lifting needs at individual wells and the energy losses associated with conversion and transmission of power across the well field.

Combined simulation–optimization models for well field development have been proposed in the literature (Varljen and Shafer 1993; McKinney and Lin 1994; Wang and Zheng 1998; Coppola et al. 2007; Fowler et al. 2008). These models typically combine a groundwater flow model with optimization routines to maximize the amount of production from a fixed set of wells or identify optimal well locations from a set of fixed (integer formulation) or nearly infinite set of possibilities available within the domain of interest (nonlinear formulation). Evolutionary programming approaches, such as the derivative free sampling methods, genetic algorithms and simulated annealing, have been used and are noted to provide better results than traditional optimization schemes (Fowler et al. 2008). In particular, simulated annealing is seen to produce similar results to the genetic algorithm but with fewer iterations (Wang and Zheng 1998). Most well field design models seek to minimize costs by minimizing the lift requirements. Recently, Madsen et al. (2009) integrated a groundwater flow and pipe network model to simulate transmission from the well field and used an enumeration strategy to determine optimal (energy efficient) well field configuration. However, the source of energy has not been explicitly considered in any of the above studies.

Based on the above discussion, it is clear that while the importance of energy optimization at well fields is explicitly recognized and the potential of using wind power for groundwater production at well fields is beneficial there are currently no models available for performing a wind-enabled water production evaluation. An integrated decision support framework that characterizes the maximal energy that can be generated from available wind resources (energy supply), along with the best way to use it in groundwater production (energy demand) through proper siting of wind turbines and water wells, has not been presented in the literature. The focus of the present study is to develop such a decision support system (DSS) framework for wind-enabled groundwater production. The proposed framework consists of two modules. The first module uses

an analytical wake model coupled with re-sampling based optimization methods for identification of optimal wind turbine siting in a wind farm. The second model uses the results from the wind farm optimization module to identify optimal locations of groundwater production wells in a well field. This latter model integrates the analytical solution for radial groundwater flow (Theis solution) in conjunction with the superposition principle and the simulated annealing (SA) optimization technique to develop best well configuration. The developed DSS is used to identify factors controlling wind-enabled water supply, and its utility is illustrated using a case-study based in San Patricio County in the coastal bend region of South Texas.

Mathematical model

Modeling wind wake fields in the presence of turbines

The Jensen multiple wake model was used in this study to simulate wake fields (Jensen 1983). This approach has been used in many wind farm optimization studies and is based on the principle of conservation of momentum and yet is parsimonious for use in practical design applications (Grady et al. 2005). To apply the simulation model, the wind turbines are assumed to be located at several sites with the coordinate of each turbine given by (x_i, y_i) . The X axis is assumed to be parallel to the predominant wind direction, which may not necessarily be the highest wind speed. The turbines in the wind farms are all assumed to have the same rotor diameter and turbine heights. Following Jensen (1983), the following expressions can be used to obtain wind velocity downstream of a turbine:

$$\pi r^2 u = \pi R^2 u_r + \pi (r^2 - R^2) u_z \tag{1}$$

$$u_r = (1 - a) u_z \tag{2}$$

$$a = 0.5 \sqrt{1 - C_T} \tag{3}$$

$$r = R + \alpha x \tag{4}$$

$$R = r_o \sqrt{\frac{1 - a}{1 - 2a}} \tag{5}$$

$$\alpha = \frac{0.5}{\ln\left(\frac{z}{z_o}\right)} \tag{6}$$

where, r is the downstream wake radius, R is the radius of the wake immediately after the rotor (downstream rotor radius), r_o is the rotor radius, u is the wind velocity at a distance x downwind of the turbine; u_r is the wind velocity immediately after the rotor; u_z is the free wind speed at the height of the turbine. The constant, α is the wake decay constant which depends upon the roughness

of the surface terrain (z_o) and turbine (rotor) height (z). From Eq. (2), the axial induction factor, a , can be seen as the percentage reduction in the wind speed from free wind speed to that behind the rotor and is a function of the thrust coefficient (C_T). The wind speed is usually measured at a reference height, z_a (typically 10 m from the ground surface) and is referred to as the ground level (ambient) wind speed. The free wind speed at any height, z can be obtained via power law scaling expressions (Turner 1972) as:

$$\frac{u_z}{u_a} = \left(\frac{z}{z_a}\right)^\beta \tag{7}$$

where, z_a is the ambient wind speed measurement height, z is the height of the rotor, u_a and u_r are wind speeds corresponding to ambient measurement height and rotor height, respectively. The exponent, β is a function of the surface roughness as well as meteorological stability conditions (Hsu et al. 1994).

The above equations describe the wind speed variation in space due to the presence of a single turbine. When there are multiple turbines, the downwind turbines will experience wakes from all upwind turbines. The wind speed experienced by a downwind turbine at location j , due to the presence of an upwind turbine, i , can be obtained by calculating the velocity deficit, vd_{ij} , as follows (Lackner and Elkinton 2007):

$$vd_{ij} = \frac{2a}{1 + \alpha \left(\frac{x_{ij}}{R}\right)^2} \tag{8}$$

where, x_{ij} is the distance between turbines i and j and the wind speed (u_j) experienced at the downwind turbine, j can be calculated as:

$$u_j = \sqrt{\sum_{i \in w(j)} (vd_{ij})^2} \tag{9}$$

where, $w(j)$ is the list of upwind turbines that affect turbine j . As can be seen from Eq. (8), the farther the upwind turbine is, the smaller will be its contribution to the overall velocity deficit and hence a smaller influence on the downwind velocity.

Once the wind velocity at each turbine is determined, the power generated by the j th turbine can be calculated as:

$$P_j = \frac{1}{2} \eta_{wt} \rho_{air} u_j^3 (\pi r_o^2) \tag{10}$$

where, P_j is the power generated by the j th turbine, η_{wt} is the efficiency of the wind turbine, and ρ_{air} is the density of the air. The density of air varies with altitude and neglecting moisture effects can be calculated using the ideal gas law as follows (Brutsaert 2005):

$$\rho_{air} = \frac{pM}{R_u T} \tag{11}$$

$$T = T_o - Lh \tag{12}$$

$$p = p_o \left(1 - \frac{Lh}{T_o}\right)^{\left(\frac{gM}{R_u L}\right)} \tag{13}$$

where, h is the height above sea level where the density is being calculated, T_o and p_o refer to standard temperature and pressure at sea level. R_u is the universal gas constant, L is the temperature lapse rate and M is the molar mass of air.

The model presented above calculates the wind power at a given turbine that is potentially experiencing wake interactions caused by upwind turbines. The total power for a given turbine network can be obtained by summing up the power generated by each turbine within the network. The efficiency of the wind farm can be calculated by taking the ratio of the total power generated for a given network configuration against the total power that could be potentially generated if the turbines did not experience any wake (i.e., they were spaced very far apart in a uniform flow field). The wind farm efficiency (η_{wf}) can be calculated as:

$$\eta_{wf} = \frac{\sum_{j=1}^J P_j}{J \times P_{theo}} \quad \text{where} \quad P_{theo} = \frac{1}{2} \eta_{wt} u_z^3 (\pi r_o^2) \tag{14}$$

It is important to recognize that the model presented above calculates wind power for a given wind direction parallel to the X axis. It is possible for winds to blow in directions other than that considered here. Therefore, coordinate transformation must first be performed such that the X axis is parallel to the wind direction under consideration using the following transformed coordinates to make the necessary distance calculations prior to using the above equations for wind power calculations.

$$\begin{bmatrix} x^* \\ y^* \end{bmatrix} = \begin{bmatrix} \cos(\theta) & -\sin(\theta) \\ \sin(\theta) & \cos(\theta) \end{bmatrix} \begin{bmatrix} x \\ y \end{bmatrix} \tag{15}$$

The transformation angle, θ , is measured in the counter-clockwise direction. If the wind speeds and the probability of their occurrence along different angles (wind speed classes) are known, then the expected power generation can be computed as follows:

$$E(P) = \sum_{m=1}^M \sum_{j=1}^J P_{j,m} p_m \tag{16}$$

where $E(P)$ is the expected power, $P_{j,m}$ is the power generated at the j th turbine under m th wind speed class and p_m is the probability of occurrence of the m th wind speed class.

Re-sampling approach to evaluate near-optimal wind turbine locations

The model presented above calculates the wind power for a given network configuration. The goal of wind farm optimization studies is to identify the locations for a given set of wind turbines that yield the maximum power. Generally, there are a finite number of locations where wind turbines can be placed within a farm. It is important that turbines are placed at least a few rotor diameters apart to not only avoid collisions but also ensure compatibility with the Jensen’s model (Vermeer et al. 2003). As the objective is to identify a subset of locations from a larger finite population, the wind farm optimization problem represents a combinatorial programming model. Classical derivative based approaches are typically not suited for combinatorial optimization models as the response surface is discrete and discontinuous. Evolutionary optimization schemes such as Genetic Algorithms (Grady et al. 2005) and particle swarm optimization (Chowdhury et al. 2012) have been adopted. In a similar spirit, a re-sampling based optimization methodology is adopted in this study. In this technique, a large number of configurations are generated by sampling without replacement and the wind power associated with each configuration is calculated. The configuration providing the maximum power is selected as the optimal wind farm layout. In a manner analogous to most evolutionary algorithms, the re-sampling technique makes random sweeps across the decision space and as such is less likely to converge to a locally optimal solution. However, the global optimality of the ideal solution cannot be directly checked. Therefore, the solution provided is interpreted as a reasonable value (if not necessarily the optimal value) of the power generated for a given set of meteorological conditions and network size.

Simulation model for establishing production-drawdown relationships

The groundwater flow equation in the radial coordinate system was used to simulate the effects of groundwater production within the study area and establish a relationship between production and drawdown. As the modeled domain is fairly small, the aquifer was assumed to be homogeneous and isotropic and represented using effective hydraulic conductivity (K) and storage coefficient (S). The mathematical model for groundwater flow in this case, is given by the following equation (Todd and Mays 2005).

$$\frac{S}{T} \frac{\partial h}{\partial t} = \frac{\partial^2 h}{\partial r^2} + \frac{1}{r} \frac{\partial h}{\partial r} \text{ and } h(x, t = 0) = h_0 \text{ and } h \rightarrow h_0 \text{ as } r \rightarrow \infty \tag{17}$$

Replacing the production (Q) by a mathematical sink leads to the well-known Theis solution which is given as:

$$h_0 - h = s = \frac{Q}{4\pi T} \int_u^\infty \frac{e^{-u}}{u} du \text{ where } u = \frac{r^2 S}{4Tt} \tag{18}$$

where, h_0 is the initial hydraulic head, h is the hydraulic head at a distance, r , from the production well at time t , and Q is the groundwater production rate. The integral in Eq. (18) is referred to as the well function in hydrologic literature. The term, s is the drawdown at the well and represents the drop in the hydraulic head from the initial condition (i.e., prior to the start of pumping).

The groundwater flow model and the solution presented in Eqs. (17) and (18) capture the production-drawdown relationship for a single well. When there are multiple wells producing in an area, the total drawdown at an observation well can be obtained via the principle of superposition, which states that the total drawdown at the observation well is the summation of drawdowns caused by production from all (multiple) wells in the area up to that point in time.

Simulated annealing model for well field optimization

Simulated annealing is a search based optimization technique that was first proposed by Kirkpatrick et al. (1983). The algorithm is inspired by the metallurgical technique of annealing wherein a solid is slowly cooled such that its structure is eventually frozen at its minimum energy configuration (Bertsimas and Tsitsiklis 1993). Simulated annealing is an iterative technique wherein during each iteration, a decision is to be made whether the system should continue to stay in its current state or move to its neighboring state. Acceptance probabilities are used to facilitate transitions to a better (lower energy) state and are controlled by a global time varying parameter called temperature which controls the rate of transitions. At early times, the temperature is high which allows both uphill and downhill transitions and thus provides a greater sweep over the solution space, which, in turn, facilitates movements away from locally optimal solutions. However, once a reasonably optimal solution is identified, the temperature becomes closer to zero and the algorithm mainly facilitates downhill descent for local refinement of the solution. The algorithm also uses several meta-heuristics to fine-tune the search process.

The optimization model used to site the wells seeks to minimize the maximum drawdowns caused at the end of a planning horizon in the production wells in order to keep the energy requirements of the lift to a minimum. The drawdown minimization requirement at the production wells will cause the wells to be spaced as far apart as possible to avoid interferences for a given level of pumping. On the other hand, the drawdown at the property boundaries must be within acceptable regulatory limits which will limit the extent to which the well field can spread at a given site. In addition, lower and upper bounds of pumping are specified at each well to ensure the required wells are in use. The optimization model can therefore be written as:

$$\text{Min: } \sum_{k=1}^K dd_{k,t} \text{ (drawdown minimization constraint)} \quad (19)$$

Subject to:

$$dd_{o,t} \leq dd_{acc} \text{ (property boundary drawdown constraint)} \quad (20)$$

$$\sum_{j=1}^J Q_j = Q_{req} \text{ (demand requirement constraint)} \quad (21)$$

$$Q_{j,\min} \leq Q_j \leq Q_{\max} \text{ (production bounds)} \quad (21)$$

$$x_{j,\min} \leq x_j \leq x_{\max} \text{ (coordinate bounds along the } X \text{ axis)} \quad (22)$$

$$y_{j,\min} \leq y_j \leq y_{\max} \text{ (coordinate bounds along the } Y \text{ axis)} \quad (23)$$

The simulated annealing algorithm is not capable of handling constraints other than the bounds on decision variables which constrain the search space. Therefore, the constraints presented in Eqs. (20) and (21) are folded into the objective function using penalty functions. A simple deviation penalty is used for the less than or equal to property boundary drawdown constraint, and a squared error penalty function is used for the equality constraint. The addition of these penalty functions results in the following modified objective function:

$$\text{Min: } \sum_{k=1}^K dd_{k,t} + c_o \sum_{o \in O} (dd_{o,t} - dd_{acc}) + c_Q \left(\sum_{j=1}^J Q_j - Q_{tot} \right)^2 \quad (24)$$

The terms c_o and c_Q represent penalties for property boundary drawdown and total production constraints. The coordinates of the production wells can be obtained by setting the total requirement to a high value to correspond to some maximum anticipated demand in the future as doing so will ensure that the wells are sufficiently spaced far apart to

cause minimal interferences at lower levels of production. While not explicit in the formulation, the primary function of the above optimization model is to identify optimal spacing of the wells within the area of interest. The model also provides the relative fraction of water that is expected to be produced by each well within the well field.

Wind energy availability (supply) and water production (demand) assessment

The optimization model presented above does not explicitly consider the power available from wind sources for lifting groundwater. The second phase of the optimization model considers this aspect by establishing an energy production curve. The curve plots the energy requirements (over a planning horizon) for lifting a known quantity of water from a given well configuration. The available energy from the wind resources is intersected with this energy production curve to obtain the achievable groundwater production. The total energy required for groundwater production is calculated as follows:

$$E_{gw} = (\rho_w g) \sum_{j=1}^J \int_0^T Q_j (EL_j - h_{j,t}) dt \quad (25)$$

where, ρ_w is the density of the water, g is the acceleration due to gravity and EL is the elevation of the land surface (measured from the same datum as the hydraulic head h) at the j th well.

Illustrative case-study

The utility of the mathematical model developed above is illustrated by applying it to assess wind-enabled water resources development in San Patricio County, TX (Fig. 1). Given the proximity to the coast, availability of wind and land resources as well as nearness to demand centers has spurred significant wind resource development in this region (SPMWD 2011). The county has a strong agricultural base and is a leading producer of Cotton and Sorghum and is home to several major industries near the Corpus Christi metropolitan area. Therefore, water demands in the region are high and expected to increase in years to come. The availability of wind resources can help considerably reduce the energy costs associated with water production, and therefore forms the basis of this case-study.

The meteorological data pertaining to wind speed and direction were collected from the Texas Crop Weather Program (CWP) near Sinton, TX. The Wind Rose plot presented in Fig. 2 indicates that the winds are

Fig. 1 Location of the study area in San Patricio County, TX

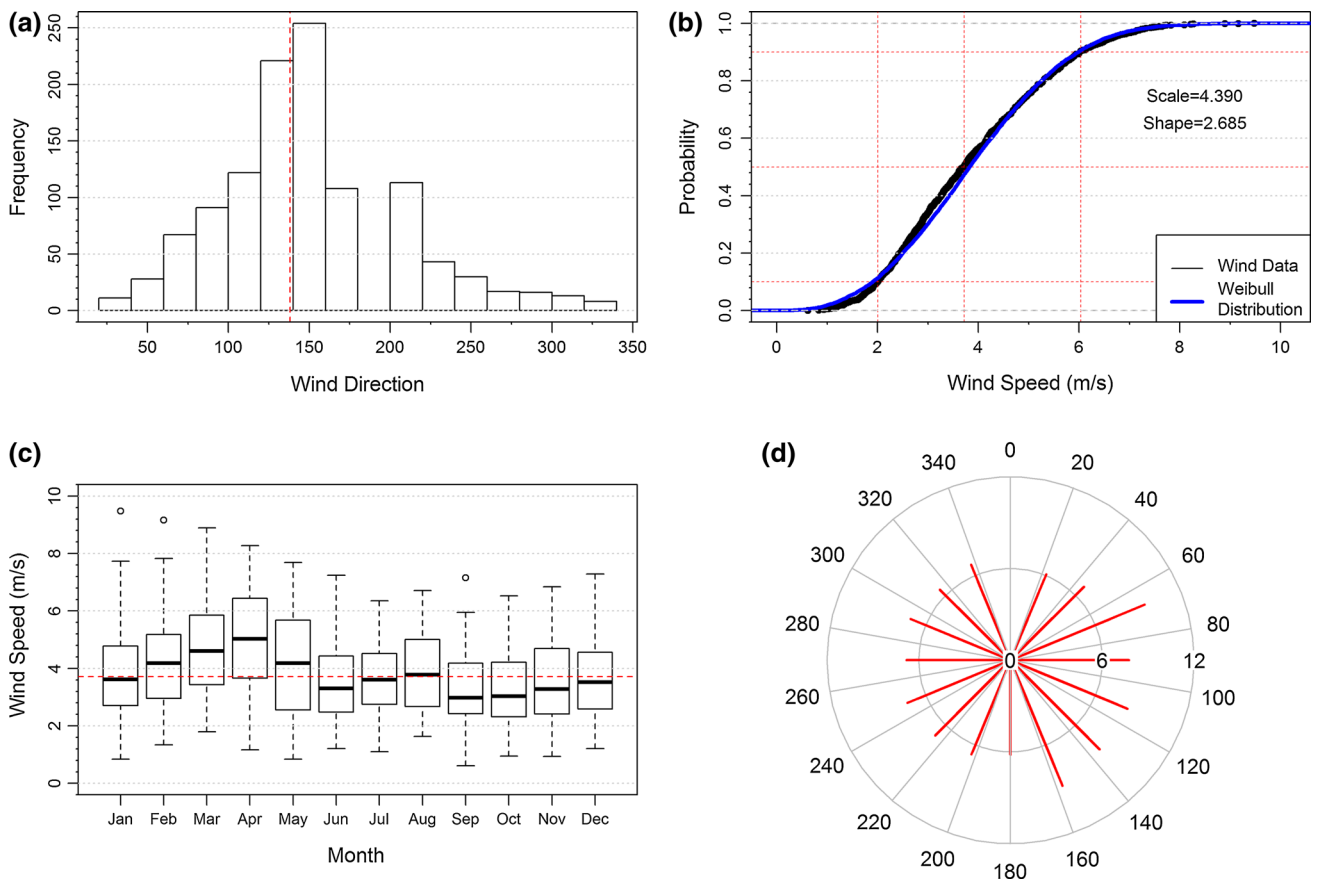
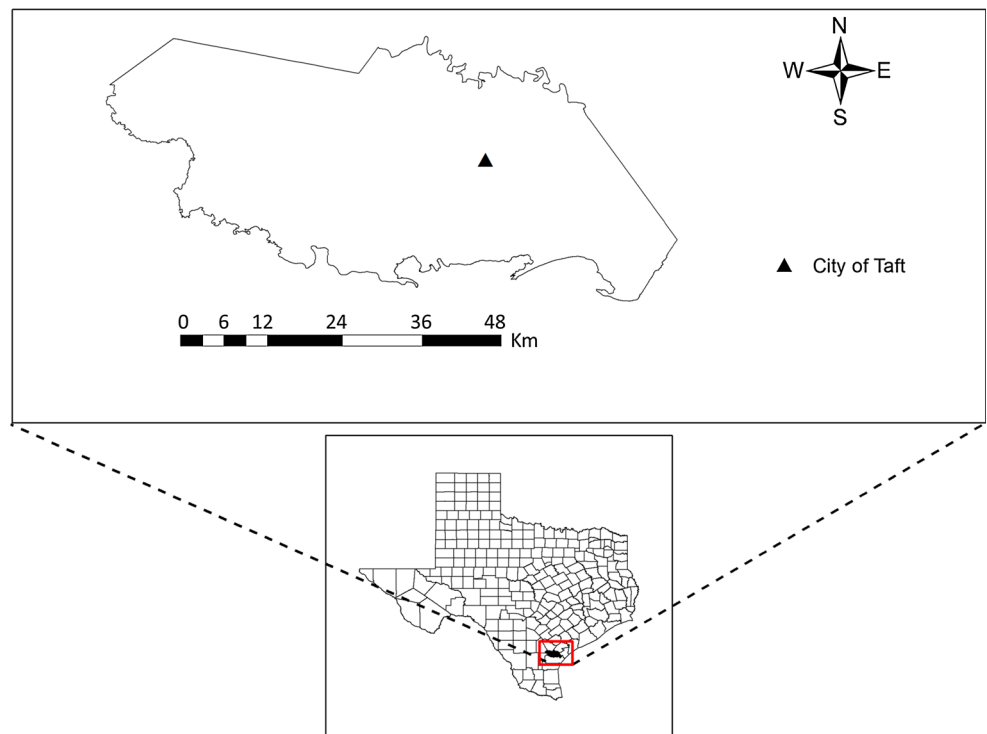


Fig. 2 Wind speed and energy characteristics at the study area

predominantly from east-southeast (from the sea towards the land) or from west southwest (land to sea). Based on the wind data, the region is in the wind power class of 3–7 and as such well suited for wind resource development (NREL 2013). The wind data fit the Weibull distribution (shape = 2.685 and scale = 4.389), which resulted in a mean value of 3.90 m/s. The temporal variability of wind speeds are also shown in Fig. 2. Wind speeds tend to be highly variable and median wind speeds tend to be higher during the months of January through May with lower wind speeds encountered during fall and winter (September–December). The variation in the median wind speeds between different months is not significant, particularly when compared to variations experienced within a month. Therefore, the median wind speed represents a reasonable value for long-term planning and to design the wind farm layout.

A small wind farm [1.6 km (1 mi) long \times 0.8 km (0.5 mi) wide] was selected in this study for illustrative purposes. The X axis of the farm was assumed to be aligned along the predominant wind direction and an assumed median wind speed of 3.75 m/s was used here to obtain conservative wind energy estimates. The median wind speeds along other major quadrants were calculated as well. A total of 98 potential turbine locations were identified within the study area to site 60 turbines, which result in 2.167×10^{27} different configurations. The hydrogeologic properties required for evaluation were obtained from data presented in Shafer and Baker (1973). The wells were assumed to tap the Evangeline aquifer and the thickness of this aquifer in the study area was ascertained from the Central Gulf Coast groundwater availability model (Chowdhury et al. 2004). The initial potentiometric head was based on groundwater monitoring data collected within the San Patricio County by the Texas Water Development Board (TWDB). All other information necessary for calculations were obtained from the literature and summarized in Table 1.

Results and discussion

Near-optimal wind turbine placement

The near-optimal wind turbine placement was obtained by performing 10,000 location re-sampling runs and identifying the optimal network configuration which yielded the most power. Figure 3 depicts the selected locations of the wind turbines with the algorithm focused on identifying the optimal turbine configuration along the predominant wind direction. This configuration yielded a power of approximately 1,700 J/s. The frequency distribution of power generated under various wind farm configurations

Table 1 Model input parameters for illustrative case-study

Parameter	Symbol	Value
Wind farm characteristics		
Wind farm length	–	1,600 (m)
Wind farm width	–	800 (m)
Minimum distance between turbines	–	120 (m)
Number of turbines	–	60
Roughness of the surface terrain	z_0	0.5
Wind turbine characteristics		
Rotor radius	r_0	20 (m)
Thrust coefficient	C_T	0.88
Turbine height	z	60 (m)
Efficiency of wind turbine	η_{wt}	50 %
Air and atmospheric characteristics		
Standard atmospheric pressure	p_0	101.325 KPa
Standard air temperature	T_0	288.15 K
Temperature lapse rate	L	0.0065 K/m
Molar mass of air	M	0.0290 Kg/mol
Groundwater and aquifer characteristics		
Storage coefficient	S	0.002
Aquifer transmissivity	T	273 m ² /days
Density of water	ρ_w	998 Kg/m ³
Physical constants		
Acceleration due to gravity	g	9.810 m/s ²
Universal gas constant	R_u	8.314 J/K/mol

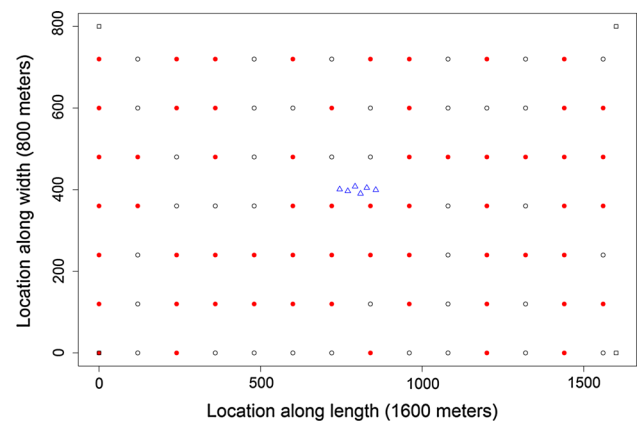


Fig. 3 Optimal wind farm and well field layout showing potential wind turbine locations (*open circles*), optimal locations of wind turbines (*closed circles*), and groundwater well locations (*triangles*)

is presented in Fig. 4, which indicates that the power generated by various configurations ranges from 1,450 J/s to nearly 1,700 J/s; therefore, optimizing wind farm operations can yield a 20 % increase in the amount of power that is generated for a given design wind speed. Albeit not optimal, the results in Fig. 4 also indicate that different wind farm configurations can yield very similar power output.

Fig. 4 Variability in wind power for evaluated wind farm layout configurations

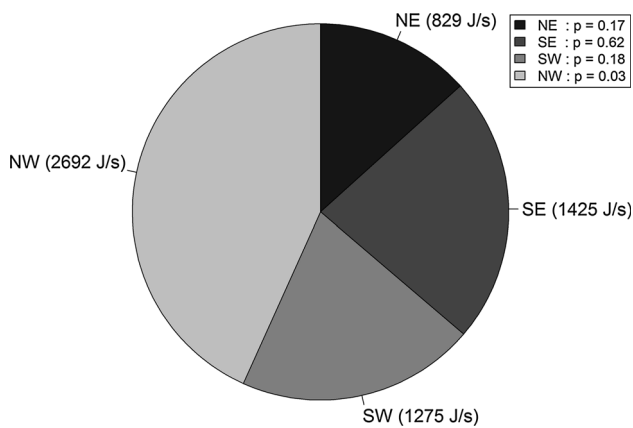
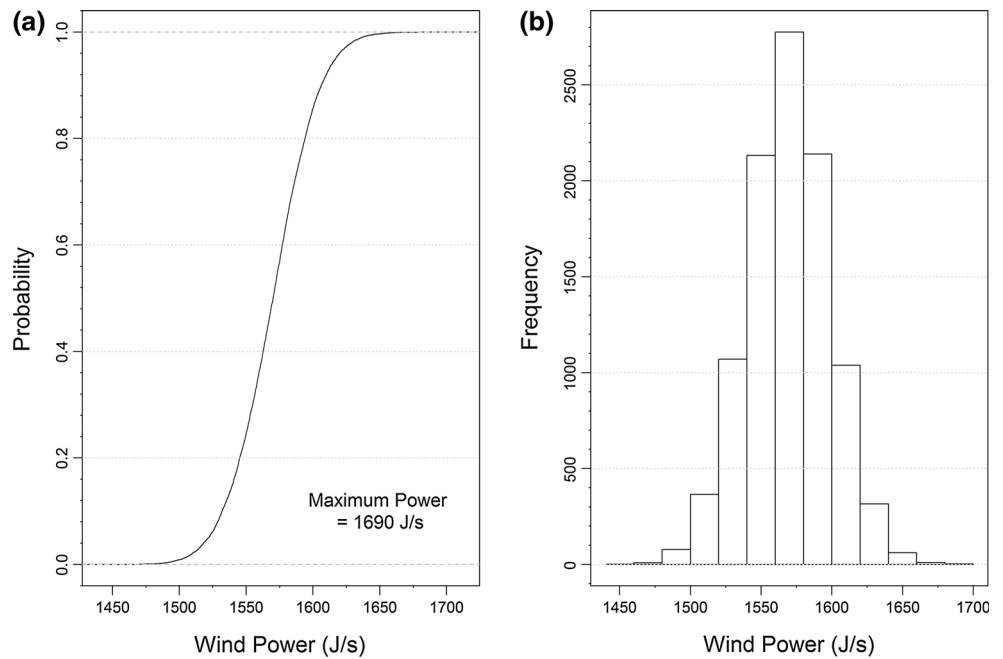


Fig. 5 Wind power generated using median wind speeds along different flow directions

Power calculations were also made for median wind speeds along other major directions and presented in Fig. 5. As can be seen, the maximum energy can be obtained when the winds are from the northwest direction. However, the probability of obtaining winds in this direction is rather low and only about 3 %. Based on the information presented in Fig. 6, the average annual wind power is calculated to be about 1,335 J/s, which corresponds to an annual energy of nearly 11,500 kWh. The efficiency of the optimized wind farm was estimated to be around 74 %, which indicates that placing the turbines within a confined space of 1.3 km² (0.5 mi²) creates wakes and reduces the kinetic energy availability in the farm. Placing the windmills very far apart, such that they are not in the wake of another turbine, increases the amount of energy that can be harnessed from available wind resources

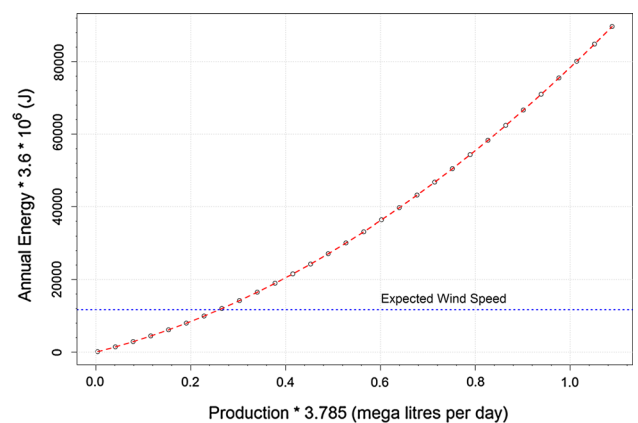


Fig. 6 Relationship between annual wind energy (KWh) and daily groundwater production (MGD)

by over 25 %. However, it is important to recognize that doing so will likely lead to other inefficiencies, particularly those associated with conversion and transmission of the electrical energy that is generated.

Optimal placement of groundwater well locations

The well network considered here consisted of six wells. The optimal locations for these wells were ascertained using the Simulated Annealing (SA) algorithm and are also depicted in Fig. 3, in the interest of brevity. The location of the wells represents a compromise between minimizing the interferences, which will cause them to be spread far apart, and ensuring that the drawdowns along the property boundaries are within acceptable limits which pushes them closer. The maximum spacing between the wells is

approximately 112 m and the minimum spacing is roughly 20 m with the mean distance between the wells being approximately 51 m. The well locations exhibit symmetry around the central diagonal of the study area. If minimizing the drawdowns at the property boundaries were the only criterion, then all wells would fall in the center of the rectangular study area as this represents the farthest distance from all boundary monitoring wells. However, the minimization of well interferences will cause the wells to move further away from each other till moving any further will cause the violation of drawdown constraints at the boundary. Repeated runs of the SA algorithm indicated that while the diagonal parallel to which the wells were placed changed directions based on the starting conditions, the distances between the wells were always the same. The fraction of production at each well hovered around the average value of 16.7 % with around ± 2 % variability among different wells. No visible trends could be discerned to characterize this variability. However, given the symmetric nature of the well placement, the expectation would be to obtain fairly uniform production at all wells such that the drawdowns are minimized to the same extent. The model results generally confirm this reasoning and any noted deviations are likely due to numerical approximations and round-off errors.

Wind power–groundwater production relationship

The relationship between annual energy requirements and the average daily groundwater production is schematically depicted in Fig. 6. The energy requirements increase exponentially with increasing production rate. For the expected annual energy generated from the wind farm [$\sim 42,120$ MJ ($\sim 11,700$ kWh)] and the assumed hydrogeological conditions at the site, the average daily groundwater production is close to 1.0 megaliters per day (0.26 MGD), which is enough to serve a community of 1,500 people. It is important to remember that wind energy is highly erratic; therefore, while the production of 1.0 MLD (0.26 MGD) can be expected on average, the daily production can exhibit considerable fluctuations. Based on the measured wind speeds, the groundwater production rate can be as high as 3.9 MLD (1 MGD) on certain days of the year, and on the other extreme the wind power could be lower than the cut-in speed of the turbine, which will result in no wind energy production, resulting in zero groundwater production.

Meteorological impacts on wind-enabled groundwater production

A detailed Monte Carlo simulation was carried out with the optimized network configuration to study how variability

in wind speeds affects groundwater production. The results presented in Fig. 7a depict the wind speed distribution that was created using 10,000 random realizations. This variability in wind speed is then propagated through the wake model to obtain the distribution of power generated as depicted in Fig. 7b. The skewness in the generated power stems from the fact that the power is a cubic function of wind speed (Fig. 7c); therefore, the effects of large wind speeds are greatly amplified relative to the small wind speeds. This stretches the abscissa and the skewness results because small wind speeds occur with a higher probability than the extreme upper values. The variability in groundwater production rates due to variable wind speeds is depicted in Fig. 7d. The relationship between power and production (Fig. 6) is noted to increase exponentially albeit at a slower rate. Based on this information and the generated power probability distribution (Fig. 7b), the groundwater production variability with wind speed exhibits a slow exponential decay as depicted in Fig. 7d. As can be seen, while the median production is about 1.0 MLD (0.25 MGD), the groundwater production varies over an order of magnitude with changing wind speeds.

The variability in wind speeds presents additional challenges to using wind for groundwater production. Firstly, the pump used for production must be capable of adapting itself to varying energy availability; and secondly, there is a need for proper water storage structures to smooth out water supply fluctuations that arise from supply variability. The variable frequency drive (VFD) pumps provide one approach to make production compatible with energy availability. Storage structures (including the option of storing the water in a shallower aquifer), which are filled when water is available and used during periods of low or no wind energy, must also be part of the design. The current analysis does not consider energy requirements associated with these operations. If the demands are to be met with a high degree of reliability, then other energy sources must also be included as a backup.

Sensitivity of hydrogeologic characteristics on wind-enabled groundwater production

A Monte Carlo simulation was carried out to evaluate how variations in transmissivity and storage coefficient affected wind-enabled groundwater production. Both transmissivity and storage coefficient were sampled from a triangular distribution, which was developed based on limited available data and understanding of the hydrogeological properties in the region. The available energy for groundwater production was held constant at the average expected value, and the amount of groundwater that can be produced was evaluated using the model. In general, increasing the transmissivity of the aquifer improves the rate at which

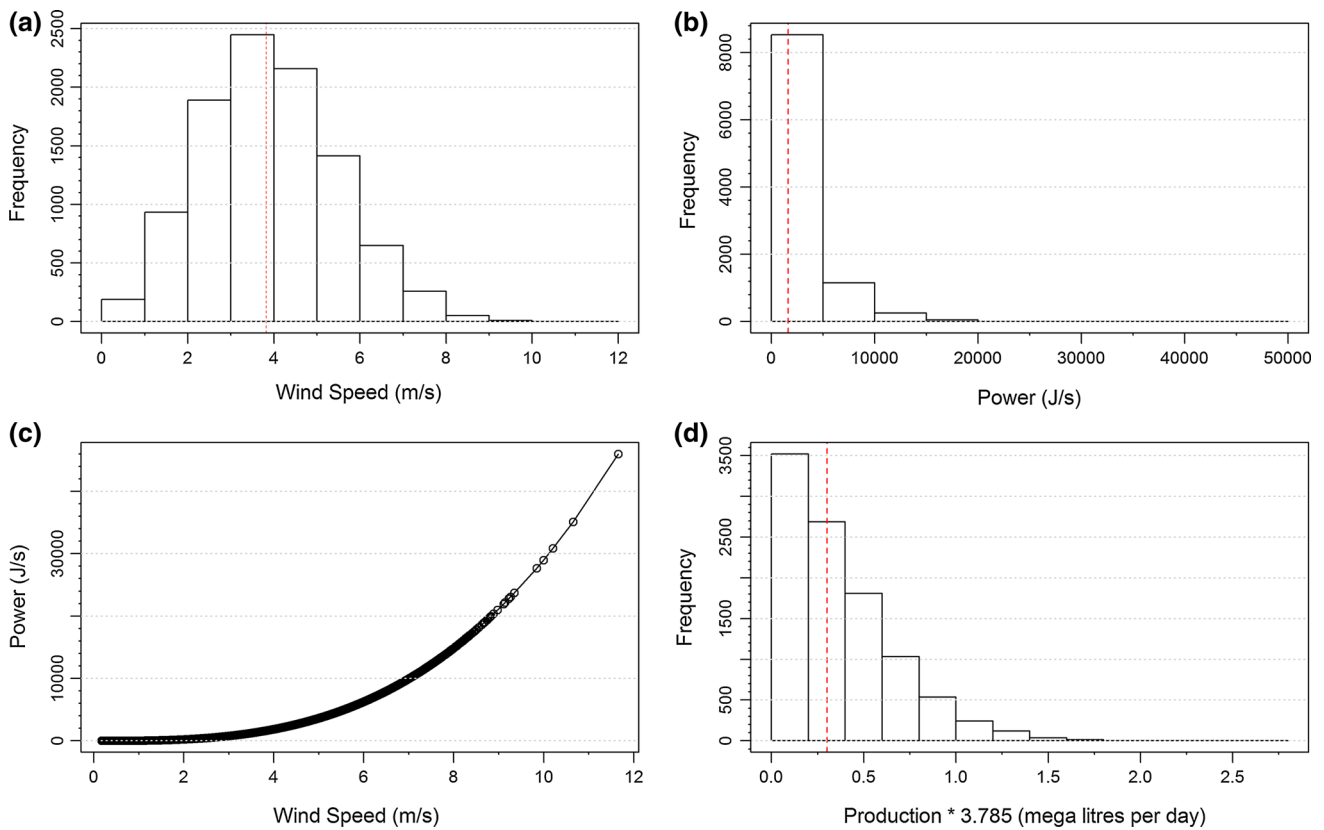


Fig. 7 Sensitivity of wind energy and groundwater production to wind speed

water flows to the well and reduces the drawdowns, which, in turn, would allow for greater extractions when all other conditions are equal. Increasing the storage coefficient results in a greater amount of extracted water coming from the aquifer in the immediate vicinity of the well, which will increase the drawdown near the well. The aquifer transmissivity and storage coefficient act in tandem; and, therefore, were varied simultaneously in the Monte Carlo simulation. Aquifer diffusivity is defined as the ratio of the transmissivity to the storage coefficient. The simulated probability distribution functions for diffusivity provides the combined effect of hydrogeological characteristics on wind-enabled groundwater production. The results from the Monte Carlo simulation are presented in Fig. 8. The generated triangular distributions exhibit skewness, which, in turn, results in a long-tailed distribution for the aquifer diffusivity. The relationship between transmissivity and groundwater production is distinctly nonlinear and the relatively steep slope in the graph suggests that aquifer transmissivity is one of the key influencing parameters, at least in the vicinity of the assumed median value. However, the increases in production are marginal when the transmissivity exceeds 600 m²/days, suggesting that hydrogeological effects are less limiting and factors other than

transmissivity (e.g., wind speeds) have a greater impact on the production rate. The combined influence of aquifer transmissivity and storage coefficient on groundwater production can be seen in Fig. 8c. More specifically, the results indicate how the nonlinear trend between transmissivity and production is influenced by the storage coefficient. The variability in produced groundwater due to uncertainty in hydrogeologic characterization is depicted in Fig. 8f. It is clear from a comparison of Figs. 7 and 8 that variability in wind has a bigger impact on groundwater production than uncertainties in hydrogeologic parameters. As such, greater benefits are gained from properly assessing winds than focusing too heavily on hydrogeologic investigations. Nonetheless, the sensitivity ranges noted do suggest that improper hydrogeological characterization, particularly under-estimation of transmissivity and storage, can cause the project to be infeasible.

Summary and conclusions

The overall goal of this study was to develop a decision support system (DSS) to evaluate wind-enabled groundwater production. The DSS is based on the integrated

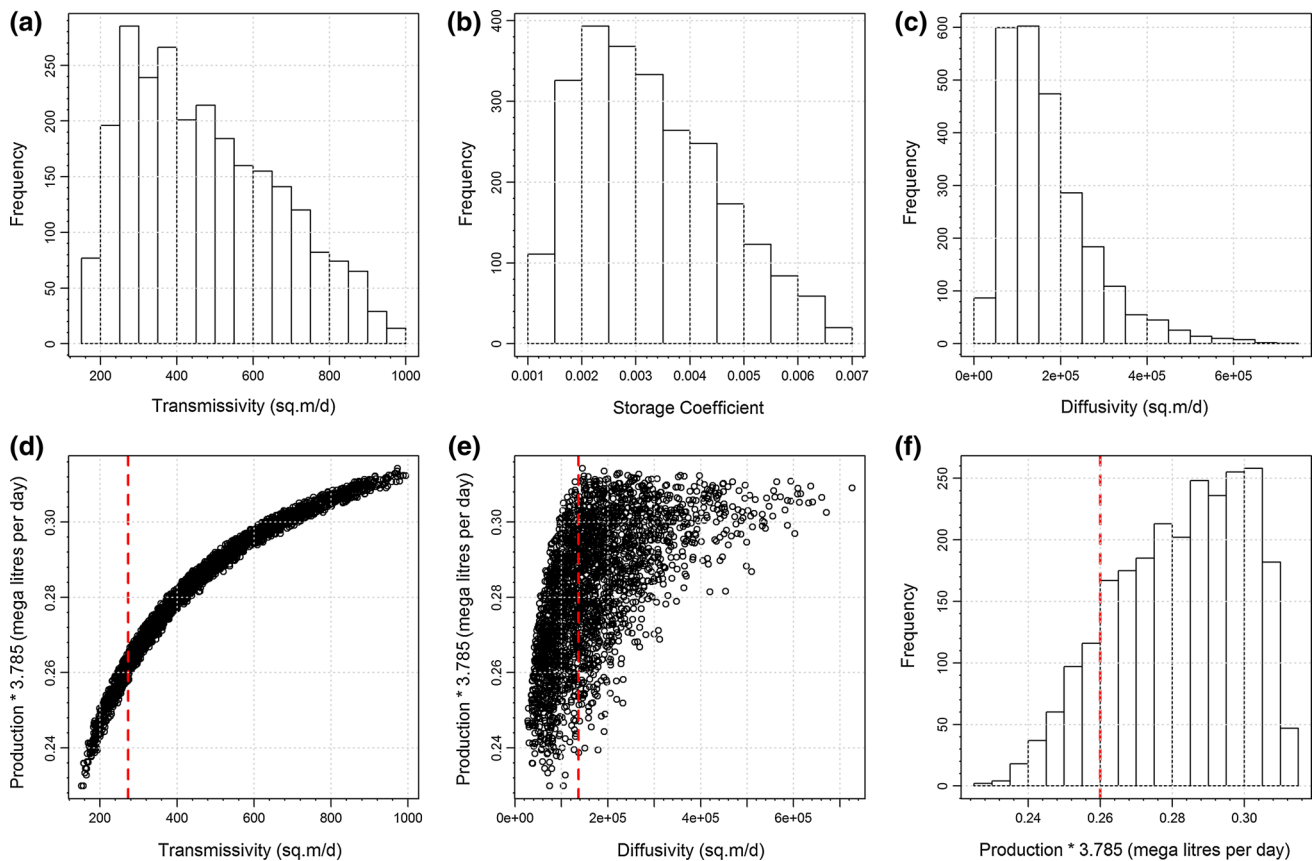


Fig. 8 Sensitivity of hydrogeologic parameters on wind-enabled groundwater production

optimization of wind resources and groundwater production. The wind power optimization model focuses on identifying the proper layout of turbines such that energy extraction from wind is optimized by minimizing the wake interactions between turbines. The groundwater well field optimization model seeks to reconcile the interference effects of placing the production wells too close against spacing them too far, which results in adverse impacts past the property of the well field and increases the costs of water collection upon pumping. The optimal energy produced by the wind farm is used to characterize the amount of groundwater that can be produced based on the amount of potential energy that is required to lift the water. A re-sampling based procedure is used to solve the combinatorial optimization model of finding optimal turbine locations. The Simulated Annealing technique is used to identify optimal well field locations and interpolation techniques are used to find the maximum groundwater production that is consistent with the available energy. The utility of the decision support system is demonstrated by applying it to evaluate an integrated wind–water farm modeled in San Patricio County, TX. A 60-turbine wind farm in a 1.3 km² (0.5 mi²) area is seen to be nearly 75 %

efficient when compared to an infinite farm that has no wake effects and produces nearly 43,200 MJ (12,000 kWh) of energy, annually. This level of power was noted to develop about 1.0 MLD (0.25 MGD) of water annually without causing excessive drawdowns at the property boundaries. A Monte Carlo sensitivity analysis was carried out to systematically evaluate the impacts of various processes and parameters on the groundwater production potential from wind farms. Wind turbine placement in the wind farm controls the amount of energy that can be extracted from prevailing winds. Sensitivity analysis on the optimized wind farm layout indicates that variability in wind speeds is a crucial parameter which has a significant impact on the groundwater production. Wind speed variability impacts the design of the water withdrawal operations. The use of variable flow drive (VFD) pumps and aquifer storage recovery (ASR) are some ways to combat the intermittency problem. While wind-enabled groundwater production is less sensitive to uncertainties in hydrogeologic parameters, improper estimation of aquifer transmissivity and storage characteristics can render wind-driven groundwater production projects infeasible.

References

- Barthelmie R (1999) The effects of atmospheric stability on coastal wind climates. *Meteorol Appl* 6(1):39–47
- Benitez LE, Benitez PC, Van Kooten GC (2008) The economics of wind power with energy storage. *Energy Econ* 30(4):1973–1989
- Bertsimas D, Tsitsiklis J (1993) Simulated annealing. *Stat Sci* 8(1):10–15
- Black M, Strbac G (2007) Value of bulk energy storage for managing wind power fluctuations. *IEEE Trans Energy Convers* 22(1):197–205
- Brutsaert W (2005) *Hydrology: an introduction*. Cambridge University Press, Cambridge
- Castronuovo ED, Lopes JAP (2004) Optimal operation and hydro storage sizing of a wind-hydro power plant. *Int J Electr Power Energy Syst* 26(10):771–778
- Chowdhury AH, Wade S, Mace RE, Ridgeway C (2004) Groundwater availability model of the central gulf coast aquifer system: numerical simulations through 1999. Texas Water Development Board, Austin
- Chowdhury S, Zhang J, Messac A, Castillo L (2012) Unrestricted wind farm layout optimization (UWFLO): investigating key factors influencing the maximum power generation. *Renew Energy* 38(1):16–30
- Coppola EA, Szidarovszky F, Davis D, Spayd S, Poulton MM, Roman E (2007) Multiobjective analysis of a public wellfield using artificial neural networks. *Ground Water* 45(1):53–61
- Elkinton CN, Manwell JF, McGowan JG (2008) Algorithms for offshore wind farm layout optimization. *Wind Eng* 32(1):67–84
- Fowler KR, Reese JP, Kees CE, Dennis J Jr, Kelley CT, Miller CT, Audet C, Booker AJ, Couture G, Darwin RW, Farthing MW, Finkel DE, Gablonsky JM, Gray G, Kolda TG (2008) Comparison of derivative-free optimization methods for groundwater supply and hydraulic capture community problems. *Adv Water Resour* 31(5):743–757
- Gonzalez JS, Gonzalez Rodriguez AG, Mora JC, Santos JR, Payan MB (2010) Optimization of wind farm turbines layout using an evolutive algorithm. *Renew Energy* 35(8):1671–1681
- Gonzalez-Longatt FM, Wall P, Regulski P, Terzija V (2012) Optimal electric network design for a large offshore wind farm based on a modified genetic algorithm approach. *IEEE Syst J* 6(1):164–172
- Grady S, Hussaini M, Abdullah M (2005) Placement of wind turbines using genetic algorithms. *Renew Energy* 30(2):259–270
- Hernandez EA, Uddameri V, Arreola MA (2013) A multi-media planning model for assessing co-located energy and desalination plants. *Environ Earth Sci*. doi:10.1007/s12665-013-2906-x
- Hsu S, Meindl EA, Gilhousen DB (1994) Determining the power-law wind-profile exponent under near-neutral stability conditions at sea. *J Appl Meteorol* 33:757–772
- Jensen NO (1983) A note on wind generator interaction. Risø National Laboratory, Roskilde
- Kirkpatrick S, Gelatt JD, Vecchi MP (1983) Optimization by simulated annealing. *Science* 220(4598):671–680
- Kusiak A, Song Z (2010) Design of wind farm layout for maximum wind energy capture. *Renew Energy* 35(3):685–694
- Lackner MA, Elkinton CN (2007) An analytical framework for offshore wind farm layout optimization. *Wind Eng* 31(1):17–31
- Madsen H, Refsgaard A, Falk AK (2009) Energy optimization of well fields. *Ground Water* 47(6):766–771
- McKinney DC, Lin MD (1994) Genetic algorithm solution of groundwater management models. *Water Resour Res* 30(6):1897–1906
- Monteiro C, Bessa R, Miranda V, Botterud A, Wang J, Conzelmann G (2009) Wind power forecasting: State-of-the-art 2009, Report ANL/DIS-10-1, 2009. Argonne National Laboratory. www.dis.anl.gov/projects/windpowerforecasting.html
- NAP (1997) Valuing ground water: economic concepts and approaches. The National Academy Press, Washington, DC
- NREL (2013) Wind resource assessment. National Renewable Energy Laboratory. http://www.nrel.gov/wind/resource_assessment.html. Accessed 5 Jan 2013
- Shafer G, Baker E Jr (1973) Ground-water resources of Kleberg Kenedy, and southern Jim Wells counties, Texas. Report 173. Texas Water Development Board, Austin
- Sophocleous M (2002) Interactions between groundwater and surface water: the state of the science. *Hydrogeol J* 10(1):52–67
- SPMWD (2011) 196 Wind turbines cranking out power. San Patricio Municipal Water District. <http://sanpatwater.com/news12.15.10.php>. Accessed 5 Jan 2013
- Todd DK, Mays LW (2005) *Groundwater hydrology* edition, 3rd edn. Wiley, New Jersey
- Turner J (1972) On the energy deficiency in self-preserving convective flows. *J Fluid Mech* 53:217–226
- Uddameri V (2007) Using statistical and artificial neural network models to forecast potentiometric levels at a deep well in South Texas. *Environ Geol* 51(6):885–895
- Uddameri V, Honnunar V (2007) Combining rough sets and GIS techniques to assess aquifer vulnerability characteristics in the semi-arid South Texas. *Environ Geol* 51(6):931–939
- Uddameri V, Singaraju S, Hernandez EA (2013) Impacts of sea-level rise and urbanization on groundwater availability and sustainability of coastal communities in semi-arid South Texas. *Environ Earth Sci*. doi:10.1007/s12665-013-2904-z
- Varljen MD, Shafer JM (1993) Coupled simulation-optimization modeling for municipal ground-water supply protection. *Ground Water* 31(3):401–409
- Vermeer L, Sørensen JN, Crespo A (2003) Wind turbine wake aerodynamics. *Prog Aerosp Sci* 39(6):467–510
- Wang M, Zheng C (1998) Ground water management optimization using genetic algorithms and simulated annealing: formulation and comparison. *JAWRA J Am Water Resour Assoc* 34(3):519–530